Plasma Chemistry and Plasma Processing, Vol. 24, No. 3, September 2004 (© 2004)

The Chemistry of Methane Remediation by a Non-thermal Atmospheric Pressure Plasma

Kirsty J. Pringle,[1,2] J. Christopher Whitehead,[1,4] Jonathan J. Wilman,[1,3] and Jinhui Wu[1]

Received August 19, 2003; revised October 19, 2003

The destruction of methane by a non-thermal plasma in atmospheric pressure gas streams of nitrogen with variable amounts of added oxygen has been investigated. The identities and concentrations of the end-products are determined by on-line FTIR spectroscopy and the plasma chemistry is interpreted using kinetic modelling. For a deposited energy of 118 kJ m^{-3}, the destruction is 12% in nitrogen decreasing monotonically to 5% in air. The major end-products are HCN and NH_3 in nitrogen and CO, CO_2, N_2O, NO and NO_2 for gas streams containing oxygen. The chemistry in pure nitrogen is predominantly due to reactions of electronically-excited nitrogen atoms, $N(^2D)$. The addition of oxygen converts the excited state nitrogen into nitrogen oxides reducing the methane destruction which then arises by O and OH reactions yielding CO and, to a lesser extent, CO_2. The modelling correctly predicts the magnitude of the methane destruction as a function of added oxygen and the concentrations of the end-products for processing in both nitrogen and air.

KEY WORDS: Non-thermal plasma; atmospheric pressure plasma; methane destruction; energy efficiency; reaction mechanism; kinetic modelling.

1. INTRODUCTION

Methane is a valuable and abundant resource being the major constituent of natural gas and is released during oil and gas production and coal mining. It is also produced by degradation processes such as landfill decomposition and a range of other natural sources. After carbon dioxide, it is the next most important gas responsible for the greenhouse effect contributing to 23% of the total greenhouse forcing. It is important therefore to minimize

[1]Department of Chemistry, University of Manchester, Manchester M13 9PL, UK.
[2]Present Address: Institute of Atmospheric Science, School of the Environment, University of Leeds, Leeds, LS2 9JT.
[3]Present Address: Element Six (UK) Ltd., 10 Bridge Avenue, Maidenhead, Berkshire, SL6 1RR.
[4]To whom correspondence should be addressed. Telephone: 0161 275 4692; fax: 0161 275 4598; e-mail: j.c.whitehead@man.ac.uk

0272-4324/04/0900-0421/0

uncontrolled emissions of methane and to utilize methane as a feedstock for other important chemicals in addition to its use as a fuel. There has been much effort devoted to the conversion of methane into methanol or higher hydrocarbons such as ethene or ethyne. It can also be converted into syngas (a mixture of CO and H_2) for use as a fuel or a source of hydrogen. However, the extreme stability of methane means that these processes are very inefficient requiring very high temperatures, the use of catalysts or some form of selective excitation of the CH_3–H bond.

Non-thermal plasma methods have been applied to these processes using both low pressure and atmospheric pressure systems. The conversion of methane into methanol with O_2, N_2O and air (sometimes with inert gases) using non-thermal plasma at atmospheric pressure has been investigated with corona, dielectric barrier and pulsed discharges often in conjunction with a catalyst.[1–5] In general, the yields of methanol are low (<10%) as are the selectivities for methanol formation (<50%). Plasma methods have been used for the production of syngas and higher hydrocarbons from the CO_2 reforming of CH_4.[6–10] Ethyne has been produced from methane with a conversion <52% and a selectivity >95% at ambient temperature and atmospheric pressure[11] and hydrocarbons as higher as C_7 have been produced in low pressure microwave discharges of methane with the aid of catalysts.[12,13] Low pressure plasma discharges of methane or methane with hydrogen are commonly used for the deposition of diamond films by CVD processes.[14–16]

The decomposition of methane in nitrogen and nitrogen/oxygen carrier gases has been studied in a variety of low pressure plasma discharges.[17–19] Several studies have developed models to describe the chemistry of such low pressure discharges.[20–24] Yamamoto and co-workers[25] have used a barium titanate packed bed plasma reactor to study methane destruction in pure nitrogen and air. In this paper, we have extended that study by investigating the process for a range of concentrations of oxygen in the carrier gas between pure nitrogen and air (20% O_2). We have also developed a model for the chemistry of the atmospheric pressure plasma processing that explains the experimental results. The operation of non-thermal plasmas at atmospheric pressure offers certain advantages over conventional technologies such as minimizing the need for complex pumping systems and eliminating corrosion problems because of the low temperature operation.

2. EXPERIMENTAL

The experimental arrangement is essentially that employed previously for our study of the plasma destruction of dichloromethane.[26] The pellet-bed reactor consists of a glass tube of 24 mm internal diameter with two

electrodes ~25 mm apart through which the gas passes. The space between the electrodes is packed with 3.5 mm diameter barium titanate beads. The diameter of the beads is chosen to allow for as large a number of beads as possible (~315), thereby maximizing the number of contact points for the formation of discharges whilst not restricting the porosity of the reactor significantly. This balances the requirements of gas flow and having as uniform a discharge as possible. An AC voltage (V_{pk-pk} = 0–20 kV) at a frequency between 10.25 and 13.25 kHz is applied between the electrodes. Using a digital storage oscilloscope (Tektronix TDS 3012), we record the current and voltage waveforms for the discharge by using a calibrated high voltage probe and measuring the current across a 1 kΩ resistor in the return earth path from the reactor. The average power of the discharge is then obtained by integrating the product of voltage and current as a function of time.

A mixed flow (~1 l min^{-1}) of zero air and nitrogen controlled by flow controllers (MKS Mass Flo) is blended with a small flow of methane giving an approximate concentration of 500 ppm of CH_4 entering the plasma reactor. The gas mixture was maintained at a pressure of 1 bar. For a gas flow of 1 l min^{-1}, the residence time in the reactor is 0.25 s. By varying the relative composition of the nitrogen/air gas flow, the oxygen composition in the gas stream could be varied in the range 0–20%. Methane was used as supplied (BOC Special Gases ≥99% purity). No attempt was made to dry the gases. The end-products of the plasma processing were monitored on-line by infrared spectroscopy (resolution ~2 cm^{-1}) using either a long-path gas cell (0–10 m, Spectra-Tech) and a FTIR spectrometer (Perkin-Elmer 1710) or an integrated gas analysis FTIR spectrometer (Gasmet DX-4010, Telmet, 9.8 m pathlength, resolution ~7.7 cm^{-1}). Stainless steel, nylon and PTFE tubing, valves and fittings of 1/4″ internal diameter were used to handle the gases as appropriate. The IR cell, the gas handling system and the plasma reactor could be evacuated to remove any traces of residual gases or moisture between experiments. No attempt was made to bake or otherwise condition the surfaces of the system.

3. RESULTS

Two separate sets of experiments were performed using the two different FTIR spectrometers. These also had different electrical power applied to the plasma reactors. In the first, the destruction of methane as a function of oxygen content in the gas stream was investigated and the end-products were qualitatively identified. This used the Perkin-Elmer spectrometer and had an electrical power input of 0.95 W. The second experiments used the Gasmet spectrometer to quantify the end-products of the processing in nitrogen and

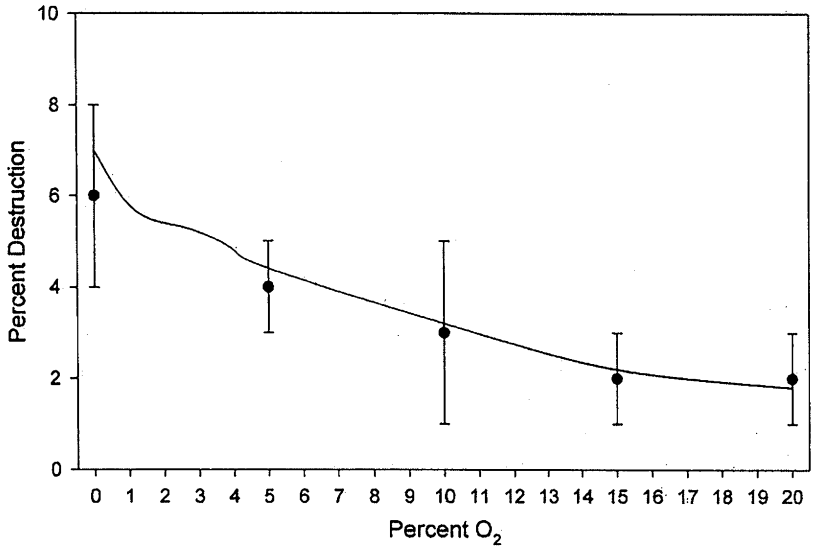

Fig. 3. A comparison of the predictions (solid line) of the kinetic model for the destruction of methane as a function of the percentage of oxygen in the feed gas with the experimental results.

as the plasma becomes more oxidising. the total amount of NO_x ($NO + NO_2$) produced increases with increasing oxygen content.

For the second series of experiments in which we quantify the end-products, we see increased destruction of methane because of the increased power. The percentage destructions are 12% in nitrogen reducing to 5% in air. The concentrations of the end-products are listed in Table I. The increased

Table I. The Percentage Destruction and End-product Concentrations for the Plasma Decomposition of 500 ppm of Methane in Nitrogen and in Air. The Concentrations of the End-products are in ppm by Volume (ppm). The Errors in the Concentrations are Typically ±5%

	Methane in nitrogen		Methane in air	
	Experiment	Model	Experiment	Model
% CH_4 destruction	12.4	13.6	5.4	5.2
HCN	36	35	0	0
NH_3	70	65	0	0
CO	3	0	30	22
CO_2	12	0	4	6
NO	5	0	452	488
NO_2	0	0	328	300
N_2O	2	0	134	110

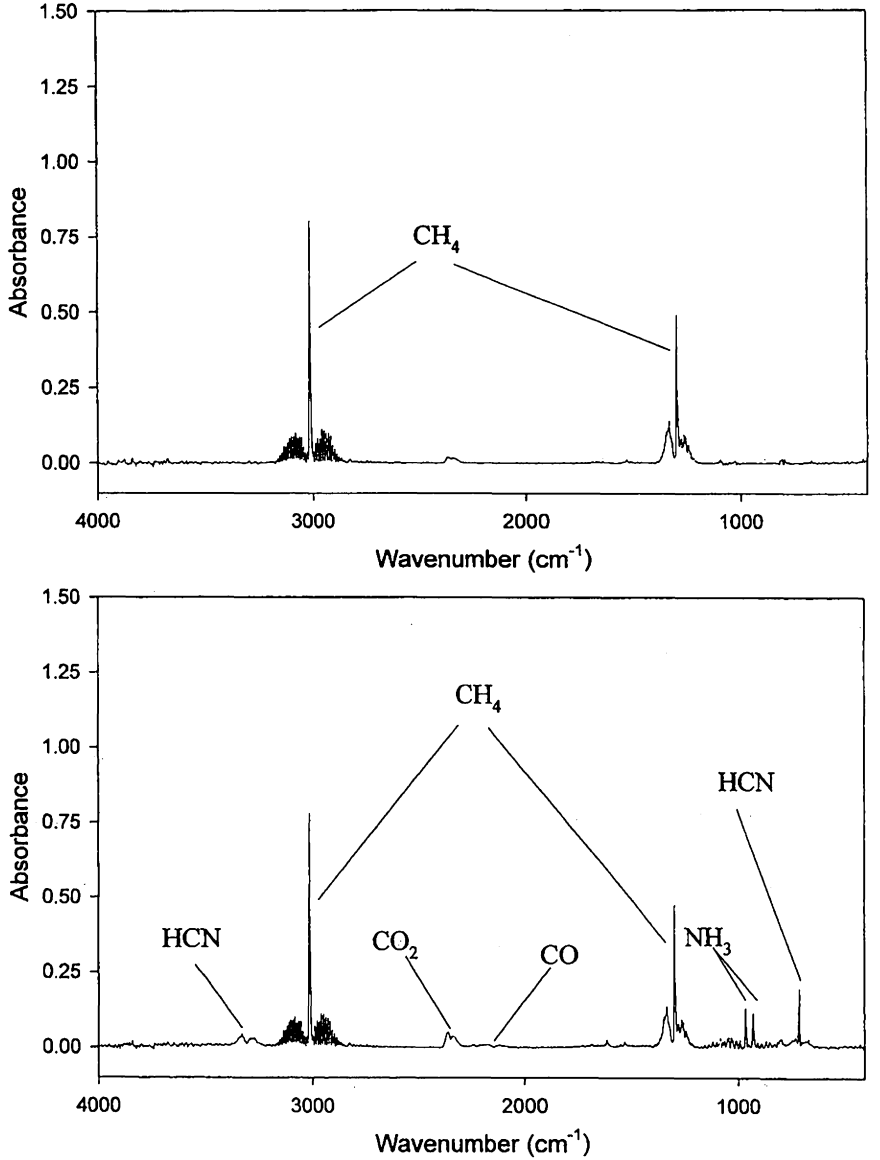

Fig. 1. Medium resolution (2 cm^{-1}) infrared spectra for an initial mixture of 500 ppm of methane in pure nitrogen at atmospheric pressure before plasma processing (upper panel) and following plasma processing (lower panel). The discharge conditions were V_{pk-pk} = 15 kV, frequency = 10.0 kHz and flow rate = 1 l min^{-1}. The path-length for the infrared gas cell was 2.12 m.

air providing additional information with which to validate the modelling. The deposited electrical power was 1.96 W in this case.

For the series of experiments performed to investigate the effect of oxygen composition (0–20%) on the plasma destruction of methane, Figs. 1 and 2 show the medium resolution IR spectra for the end-products of the plasma processing of 500 ppm of CH_4 in pure N_2 and in air (20% O_2), respectively. The spectra were assigned and the measured absorbances converted into concentrations using standard gas-phase spectral compilations.[27] In the case of destruction in pure nitrogen, we see only the production of HCN and NH_3 whilst CO, CO_2, NO, NO_2 and N_2O are detected in the presence of oxygen in the gas stream. Figure 3 shows the percentage destruction of CH_4 as a function of oxygen compositions in the gas stream. The degree of destruction of the methane decreases monotonically with increasing oxygen content from 6% in pure nitrogen to 2% in air (20% O_2). This contrasts with the finding for the processing of dichloromethane where there was a maximum in the destruction efficiency at 1–3% O_2.[26] There is significant production of nitrogen oxides when the carrier gas contains any oxygen. The amounts of N_2O and NO remain roughly constant with changing oxygen content greater than 5% but the amount of NO_2 increases

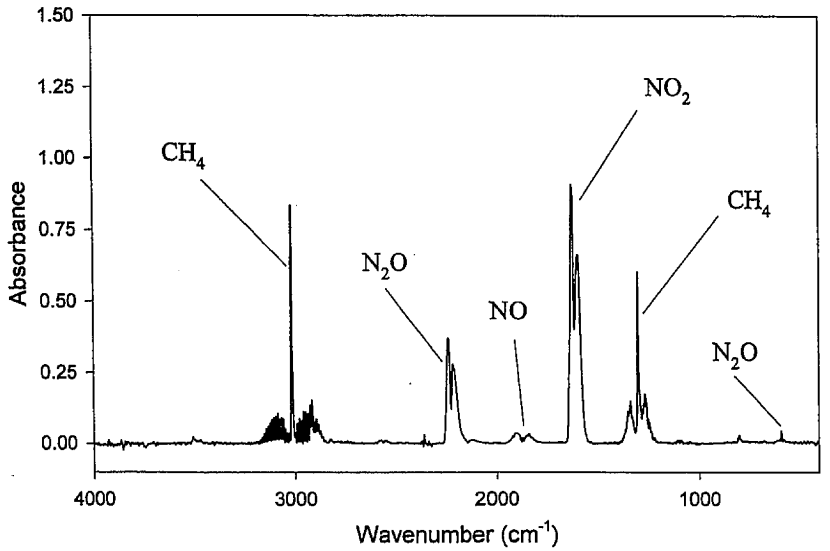

Fig. 2. Medium resolution (2 cm^{-1}) infrared spectra for an initial mixture of 500 ppm methane in a gas stream of air (20% O_2, 80% N_2) at atmospheric pressure after processing in a dielectric pellet-bed reactor. The discharge conditions were V_{pk-pk} = 15 kV, frequency = 10.0 kHz and flow rate = 1 l min^{-1}. The path-length for the infrared gas cell was 2.12 m.

power in these experiments also means that the packed bed runs at a slightly elevated temperature of 430 K.

Analysis of the electrical power dissipated in the reactor shows that the deposited energy density is 57 and 118 kJ m^{-3} for the first and second series of experiments, respectively. This means that the destruction of methane is at an energy cost of 500 and 720 eV per molecule for the destruction in nitrogen in each case.

4. DISCUSSION

4.1. Comparison with Previous Studies

There have been few previous investigations of the non-thermal, atmospheric pressure plasma processing of methane. Okumoto *et al.*[2] investigated the direct synthesis of methanol in mixtures of 94–98% CH_4 in O_2. They found that 2% of the methane could be removed with a selectivity of 30% for methanol production and that this could be enhanced by the addition of a catalyst. Further investigations of the discharge characteristics by the same group[4] showed that the energy required to produce a methanol molecule is 104 eV. The group of Yamamoto[25] have studied the decomposition of methane in air and nitrogen using a $BaTiO_3$ plasma reactor.

Differences in the reactor design and lower gas flows meant that the residence time (3.6 s) was longer than in the present study. For 1000 ppm of methane in air, up to 30% of the methane was decomposed with the products of the decomposition being CO and CO_2 with CO in excess. Several hundred ppm of NO_x and N_2O were also produced. It was observed that whilst the concentration of N_2O remained constant, the amount of NO_x increased with increasing O_2 content. Dissociation in nitrogen produced HCN and NH_3 as the major end-products with a very small amount of acetylene, C_2H_2. Further work by Yamamoto[28] shows that destruction of methane is more efficient in nitrogen than in air by about a factor of two. All of these findings accord broadly with our own results.

4.2. Modelling of the Plasma Processing

None of the previous studies have discussed the reaction chemistry taking place during these atmospheric pressure, plasma processing experiments. In contrast, there has been considerable activity to determine reaction mechanisms for low pressure methane plasmas involving pure methane,[29] methane in oxygen[16,17,23,24] and in nitrogen.[20–22] We have extended our computer-based, kinetic model of atmospheric pressure plasma processing that was applied to the decomposition of dichloromethane[26] to describe the

plasma destruction of methane as an aid to understanding the reaction chemistry.

The chemistry involved in the plasma processing was modelled using the chemical kinetics package, CHEMKIN-II.[30] Following the method of Gentile and Kushner,[31,32] we assume that there is uniform processing of the gas as it passes through the reactor. During each half-cycle, the micro-discharge current pulses create active species which then go on to initiate or continue the chemistry. In our model, a fresh supply of the active species is injected into the reaction mixture at each pulse and the chemistry is allowed to continue until the next pulse. The concentrations of species added per pulse are determined from the G values calculated by the ELENDIF programme[33] in conjunction with the relevant electron–molecule collision cross-sections and the experimentally determined value for the electrical power deposited in the plasma. After a time of 0.25 s, the residence time in the plasma reactor, processing ceases and the final concentrations are output. This model is based on volume averaged quantities. In fact, the microstreamers are filamentary in form with diameters of approximately ten or hundreds of microns. Thus the radicals are initially produced in confined regions rather than uniformly throughout the gas volume. However, of all of the designs of dielectric barrier plasma reactors, the packed pellet-bed offers one in which the number of microstreamers is maximized and the volume of free gas is minimized. For this design, we feel that the volume averaged model will provide a reasonably accurate description of the plasma processing.

In the plasma, the gas is at near ambient temperature and the electron impact dissociation and excitation produces a range of atoms and molecules including $O(^3P$ and $^1D)$, $O_2(a^1\Delta)$, $N(^4S, ^2D, ^2P)$ and $N_2(A^3\Sigma_u^+)$. The relative concentrations of these species have been calculated previously[26] for the different oxygen concentrations in the carrier gas. Oxygen and nitrogen molecules are the major species in the gas streams and the chemistry initiated by the plasma discharge is dominated by oxygen and nitrogen species. Methane is present in the gas stream at much lower concentrations and it is unlikely that direct decomposition of methane by electron impact plays a major role in its decomposition chemistry. Although the C–H bond strength in methane is only 4.51 eV, the threshold for dissociation by electron impact is considerably higher at 9 eV. The cross section for electron-impact dissociation of methane[34] has a maximum at 20–30 eV and falls rapidly to the threshold with decreasing electron energy. For plasmas of the type employed in this study where the reduced electric field strength, E/N, is in the range 75–150 Td ($1\ \text{Td} = 1\times10^{-17}\ \text{V cm}^2$), the electron energy distributions peak at very low energies with mean energies in the range 1.7–3.8 eV.[35,36] This means that the fraction of electrons in the plasma discharge having sufficient

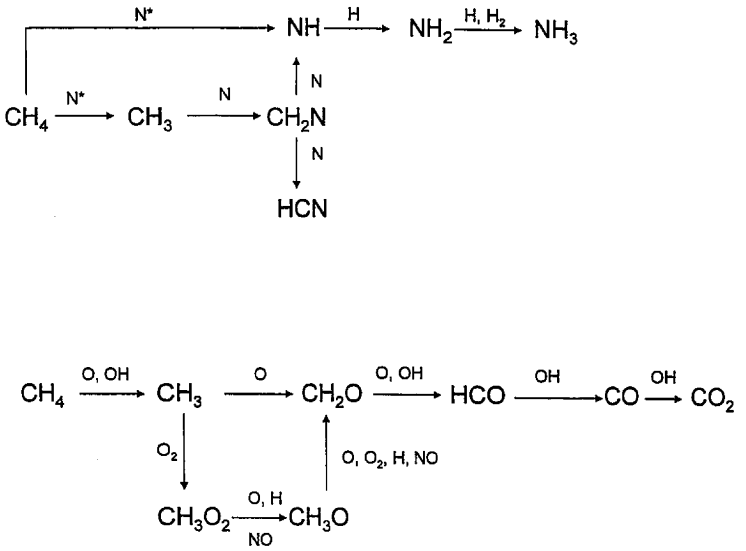

Fig. 4. A schematic representation of the reaction chemistry for the non-thermal, atmospheric pressure, plasma destruction of methane in pure nitrogen (upper panel) and in air (lower panel).

energy to directly dissociate methane to give methyl radicals is very small and decomposition of methane by this route can be ignored.

We now discuss a possible chemical mechanism for the plasma decomposition of methane with reference to the pathways displayed in Fig. 4. In pure nitrogen, the decomposition of CH_4 is likely to come about from reaction with electronically-excited, metastable nitrogen molecules, $N_2(A^3\Sigma_u^+)$, or nitrogen atoms, $N(^2D)$, formed in the discharge giving a methyl radical in both cases

$$N_2(A^3\Sigma_u^+) + CH_4 \rightarrow N_2(X^1\Sigma_g^+) + CH_3 + H \quad (1)$$

$$N(^2D) + CH_4 \rightarrow NH + CH_3 \quad (2)$$

These reactions ($k_1 = 3.2\times10^{-15}$ cm^3 s^{-1}[37], $k_2 = 1.5\times10^{-12}$ cm^3 s^{-1}[38]) are invoked as initial steps in the modelling of a low pressure CH_4/N_2 microwave plasma by Legrand *et al.*[20–22] In their modelling, they use the same value for both rate constants (1.5×10^{-12} cm^3 s^{-1}).[21] Whilst this value is appropriate for reaction (2), it is a significant overestimate for reaction (1). Although calculations[26] indicate that the yield of $N_2(A^3\Sigma_u^+)$ is about three times that of $N(^2D)$ in an atmospheric plasma of pure nitrogen, it is clear that the major route for the decomposition of methane is via reaction (2)

involving hydrogen atom abstraction yielding NH. Figure 4 shows that this is then converted into one of the observed end-products, NH_3, by reaction with hydrogen. The methyl radicals formed in reaction (2) react with further nitrogen atoms to form either CH_2N[39] which is rapidly converted into a NH radical and HCN, the other end-product, by nitrogen atom reactions.

The experimental observation is that NH_3 and HCN are formed in approximate ratio of 2:1 which is accounted for in Fig. 4 where it can be seen that decomposition of CH_4 by N atoms leads to two NH radicals for every HCN molecule produced. However, the full conversion of NH radicals into ammonia requires an adequate supply of hydrogen atoms. In the modelling, we investigated various sources for the H atoms including the reactions of N_2* with hydrocarbon radicals such as CH_3, CH_2 and CH as suggested by Legrand *et al.*[20–22] We found that their quoted rate constants were up to 10^6 times too large to give agreement between model and experiment and that this was a minor process. Instead, we found that the following sequence of reactions gave an adequate supply of H atoms to provide the observed yield of both NH_3 and HCN.

$$N^* + CH_3 \rightarrow N + CH_2 + H \quad (3)$$

$$N^* + CH_2 \rightarrow N + CH + H \quad (4)$$

$$CH_3 + H \rightarrow CH_4 \quad (5)$$

The results of the modelling for the processing in nitrogen are compared with the experimental results in Table I where agreement can be seen to be within experimental error.

The model cannot account for the production of the oxygen containing species (CO, CO_2, NO and N_2O) found in the experiment despite the processing being performed in pure nitrogen. Ogata *et al.*[25] have suggested that lattice oxygen species in the $BaTiO_3$ beads may play an important role in the formation of the NO_x and N_2O implying that the mechanism of their production involves both gas-phase and surface reactions. A supply of oxygen and any subsequent heterogeneous processes are not included in our modelling although there is evidence from studies of the plasma-assisted catalysis of NO_x and hydrocarbon mixtures that the nature of the packing material in the plasma bed does play a role in the outcome of the plasma processing.[40] It is likely that the hydrocarbon radicals formed in reactions (3) and (4) are oxidized to give the small amounts CO and CO_2 that we observe.

In the presence of 1% or more oxygen, we observe a change in the mechanism and there is no further production of HCN and NH_3. This arises because the excited state nitrogen atoms can now react with molecular

oxygen to form NO which is further oxidized to NO_2 giving the source of NO_x observed in this study

$$N^*(^2D) + O_2 \rightarrow NO + O \tag{6}$$

This occurs in preference to reaction (2) because of the significantly larger concentration of molecular oxygen than methane (10,000 ppm compared to 500 ppm for 1% O_2) and the slightly greater value for the rate constant ($k_6 = 6.3 \times 10^{-12}$ cm^3 s^{-1}[38]). The metastable triplet A state of nitrogen also reacts much more rapidly with molecular oxygen than with methane both because of the increased concentration effect and also because of a larger rate constant (2.4×10^{-12} cm^3 s^{-1}[37]). This reaction is a source of nitrous oxide, N_2O, in the system

$$N_2(A^3\Sigma_u^+) + O_2 \rightarrow N_2O + O \tag{7}$$

In the presence of oxygen, methyl radicals can also be formed by the reaction of methane with atomic oxygen

$$O(^3P, ^1D) + CH_4 \rightarrow OH + CH_3 \tag{8}$$

($k_8 = 1\text{–}4 \times 10^{-15}$ and 1.5×10^{-10} cm^3 s^{-1} for $O(^3P)$ and $O(^1D)$, respectively at 430 K[41]) but there is a lower yield of O atoms in the discharge compared with the electronically-excited states of atomic and molecular nitrogen in pure nitrogen. This transition from methyl radicals produced by N atoms in reaction (2) in pure nitrogen to their production by oxygen atoms in reaction (7) accounts for the reduction in destruction efficiency with increasing oxygen content of the feed gas as displayed in Fig. 3. Further reduction also arises because increasing the oxygen content of the feed gas mixture shifts the electron energy distribution to lower energies favoring vibrational excitation of the oxygen rather than dissociation.[42] The destruction of the methane continues in the presence of oxygen, as the methyl radicals participate in a chain of oxidation reactions that proceed in a standard way for methane combustion via methoxy radicals and formaldehyde to ultimately yield CO and CO_2 as indicated in Fig. 4. As the oxidation continues, the concentration of OH radicals builds up providing a more efficient route for the conversion of methane into methyl radicals

$$OH + CH_4 \rightarrow H_2O + CH_3 \tag{9}$$

($k_9 = 1.5 \times 10^{-13}$ cm^3 s^{-1} at 430 K[41]).

We have modelled the plasma destruction of methane as a function of oxygen concentration using the reaction mechanisms outlined in Fig. 4 with additional processes from the literature[20–24] (55 species and 200 reactions)

and the rate constants given above and in standard compilations.[41] The comparison of the model predictions and our experimental results is given in Fig. 3 and shows good agreement in terms both of the magnitude of the destruction and the trend with changing oxygen concentration. The model also confirms that all the methane is converted into CO or CO_2 and that production of CO dominates over CO_2 (see the comparison in Table I) suggesting that (8) oxidation of CO is incomplete under our plasma conditions.

Experiment shows that the mechanism by which the oxides of nitrogen are formed in the plasma are largely independent of the presence of methane. The yields of NO, NO_2 and N_2O in an air plasma with and without methane are the same to within experimental error. NO and N_2O are produced by reactions (7) and (8). Further reactions such as

$$O + NO + M \rightarrow NO_2 + M \tag{10}$$

$$O + NO_2 \rightarrow NO + O_2 \tag{11}$$

$$NO + O_3 \rightarrow NO_2 + O_2 \tag{12}$$

$$N + NO \rightarrow N_2 + O \tag{13}$$

are responsible for the formation of NO_2 and the final concentrations of NO_x. The result of the modelling of the NO_x and N_2O concentrations is compared with the values derived from experiment in Table I where it can be seen that there is agreement to within experimental error.

In systems with hydrocarbons, there is an additional reaction that converts NO into NO_2 by reaction with a peroxyradical (HO_2 or CH_3O_2)

$$NO + RO_2 \rightarrow NO_2 + RO \tag{14}$$

Such reactions play an important role in the treatment of exhaust gas streams with higher hydrocarbons[43] and increase the ratio of NO_2 to NO. However, in the present experiments there is no difference in the ratio of NO_2 to NO concentrations for processing in air with or without methane within experimental error.

5. CONCLUSIONS

We have presented a chemical mechanism for the non-thermal, atmospheric pressure plasma destruction of methane in feed gases with varying oxygen content from pure nitrogen to air. In pure nitrogen, the products are

HCN and NH_3 whilst CO, CO_2, NO, NO_2 and N_2O are detected with the presence of oxygen in the gas stream. The modelling of the plasma processing correctly predicts the magnitude of the methane destruction, its decrease with increasing oxygen and the yields of the end-products for processing in both nitrogen and air. The conversion of methane into hydrogen cyanide and ammonia in the absence of oxygen may be of significance. These end-products could be recovered and used as valuable feedstocks for the production of plastics and agrochemicals. It is obviously not desirable to produce large quantities of NO_x as an end-product of the plasma processing as is observed in the presence of oxygen and a hybrid plasma-assisted catalyst scheme using, for example, a metal oxide catalyst[44] might be needed to remove these species. We have also determined for the first time the energy consumption for the plasma remediation of methane in a $BaTiO_3$ packed bed reactor allowing the economic feasibility of such processing to be assessed.

ACKNOWLEDGMENT

We acknowledge support of this work by EPSRC and also AEA Technology plc who provided a CASE studentship for J.J.W.

REFERENCES

1. L. M. Zhou, B. Xue, U. Kogelschatz, and B. Eliasson, *Plasma Chem. Plasma Proc.* **18**, 375 (1998).
2. M. Okumoto, B. S. Rajanianth, S. Katsura, and A. Mizuno, *IEEE Trans. Ind. Appl.* **34**, 940 (1998).
3. M. Okumoto, Z. Su, S. Katsura, and A. Mizuno, *IEEE Trans. Ind. Appl.* **35**, 1205 (1999).
4. S. L. Yao, T. Takemoto, F. Ouyang, A. Nakayama, E. Suzuki, A. Mizuno, and M. Okumoto, *Energy Fuels* **14**, 459 (2000).
5. H. Matsumoto, S. Tanabe, K. Okitsu, Y. Hayashi, and S. L. Suib, *J. Phys. Chem. A* **105**, 5304 (2001).
6. L. Bromberg, D. R. Cohn, A. Rabinovich, C. O'Brien, and S. Hochgreb, *Energy Fuels* **12**, 11 (1998).
7. L. M. Zhou, B. Xue, U. Kogelschatz, and B. Eliasson, *Energy Fuels* **12**, 1191 (1998).
8. B. Eliasson, C. Liu, and U. Kogelschatz, *Ind. Eng. Chem. Res.* **39**, 1221 (2000).
9. M. Kraus, B. Eliasson, U. Kogelschatz, and A. Wokaun, *Phys. Chem. Chem. Phys.* **3**, 294 (2001).
10. K. Zhang, U. Kogelschatz, and B. Eliasson, *Energy Fuels* **15**, 395 (2001).
11. S. Kado, Y. Sekine, and K. Fujimoto, *Chem. Commun.*, 2485 (1999).
12. C. Marún, S. L. Suib, M. Dery, J. B. Harrison, and K. Kablaoui, *J. Phys. Chem.* **100**, 17866 (1996).
13. C. Marún, L. D. Conde, and S. L. Suib, *J. Phys. Chem. A* **103**, 4332 (1999).
14. T. Fujii and M. Kareev, *J. Appl. Phys.* **89**, 2543 (2001).
15. D. Liu, T. Ma, S. Yu, Y. Xu, and X. Yang, *J. Phys. D: Appl. Phys.* **34**, 1651 (2001).
16. M. N. R. Ashfold, P. W. May, J. R. Petherbridge, K. N. Rosser, J. A. Smith, Y. A. Mankelevich, and N. V. Suetin, *Phys. Chem. Chem. Phys.* **3**, 3471 (2001).

17. D. E. Tevault, *Plasma Chem. Plasma Proc.* **5**, 369 (1985).
18. C. D. Pintassilgo, J. Loureiro, G. Cernogora, and M. Touzeau, *Plasma Sources Sci. Technol.* **8**, 463 (1999).
19. M. Kareev, M. Sablier, and T. Fujii, *J. Phys. Chem. A* **104**, 7218 (2000).
20. J.-C. Legrand, A.-M. Diamy, R. Hrach, and V. Hrachová, *Vacuum* **48**, 671 (1997).
21. J.-C. Legrand, A.-M. Diamy, R. Hrach, and V. Hrachová, *Vacuum* **50**, 491 (1998).
22. J.-C. Legrand, A.-M. Diamy, R. Hrach, and V. Hrachová, *Vacuum* **52**, 27 (1999).
23. J. Röpcke, L. Mechold, M. Käning, W. Y. Fan, and P. B. Davies, *Plasma Chem. Plasma Proc.* **19**, 395 (1999).
24. W. Y. Fan, P. F. Knewstubb, M. Käning, L. Mechold, J. Röpcke, and P. B. Davies, *J. Phys. Chem. A* **103**, 4118 (1999).
25. A. Ogata, K. Mizuno, S. Kushiyama, and T. Yamamoto, *Plasma Chem. Plasma Proc.* **18**, 363 (1998).
26. C. Fitzsimmons, F. Ismail, J. C. Whitehead, and J. J. Wilman, *J. Phys. Chem. A* **104**, 6032 (2000).
27. P. L. Hanst and S. T. Hanst, *Infrared Spectra for Quantitative Analysis of Gases*, Infrared Analysis, Anaheim, CA (1996).
28. T. Yamamoto, *J. Haz. Mat.* **B67**, 165 (1999).
29. P. Jemmer, *Math. Comp. Mod.* **30**, 61 (1999).
30. R. J. Kee, F. M. Rupley, and J. A. Miller, Chemkin-II: A Fortran Chemical Kinetics Package for the Analysis of Gas Phase Chemical Kinetics, Sandia National Laboratory (1991).
31. A. C. Gentile and M. J. Kushner, *J. Appl. Phys.* **78**, 2074 (1995).
32. A. C. Gentile and M. J. Kushner, *J. Appl. Phys.* **78**, 2977 (1995).
33. W. L. Morgan and B. M. Penetrante, *Comp. Phys. Comm.* **58**, 127 (1990).
34. T. Nakano, H. Toyoda, and H. Sugai, *Jap. J. Appl. Phys.* **30**, 2908 (1991).
35. C. Fitzsimmons, J. T. Shawcross, and J. C. Whitehead, *J. Phys. D: Appl. Phys.* **32**, 1136 (1999).
36. J. Li, W. Sun, B. Pashaie, and S. K. Dhali, *IEEE Trans. Plasma Sci.* **23**, 672 (1995).
37. M. F. Golde, *Int. J. Chem. Kin.* **20**, 75 (1988).
38. K. Schofield, *J. Phys. Chem. Ref. Data* **8**, 723 (1979).
39. G. Marsden, F. L. Nesbitt, D. F. Nava, W. A. Payne, and L. J. Stief, *J. Phys. Chem.* **93**, 5769 (1989).
40. A. Ogata, K. Yamanouchi, K. Mizuno, S. Kushiyama, and T. Yamamoto, *IEEE Trans. Ind. Appl.* **35**, 1289 (1999).
41. W. G. Mallard, F. Westley, J. T. Herron, R. F. Hampson, and D. H. Frizzell, NIST Chemical Kinetics Database; Windows Version 2Q98 edition; U.S. Department of Commerce, National Institute of Standards and Technology, Gaithersburg (1998).
42. H. R. Snyder and G. K. Anderson, *IEEE Trans. Plasma Sci.* **26**, 1695 (1998).
43. A. R. Martin, J. T. Shawcross, and J. C. Whitehead, *J. Phys. D: Appl. Phys.*, **37**, 42 (2004).
44. J. Hoard, T. J. Wallington, J. C. Ball, M. D. Hurley, and K. Wodzisz, *Env. Sci. Tech.* **33**, 3427 (1999).